

Intrinsic diffraction losses in photonic crystal waveguides with line defects

Lucio Claudio Andreani^{a)} and Mario Agio

INFN and Dipartimento di Fisica "A. Volta," Università di Pavia, Via Bassi 6, 27100 Pavia, Italy

(Received 7 June 2002; accepted 30 January 2003)

Intrinsic diffraction losses of linear defect modes in photonic crystal slabs are calculated for membrane-type waveguides with strong refractive index contrast. In the frequency region of high group velocity of the defect mode, the radiative losses increase with the air fraction of the lattice and decrease on increasing the channel width or the slab thickness. Close to a mini-gap in the mode dispersion, a complex frequency dependence of the losses is found. The calculated losses agree well with those measured in a Si slab [M. Lončar *et al.*, Appl. Phys. Lett. **80**, 1689 (2002)]. © 2003 American Institute of Physics. [DOI: 10.1063/1.1564295]

Planar photonic crystal (PC) waveguides, or PC slabs, are extensively investigated in view of the realization of integrated optical interconnects.^{1–16} In these systems, a few photonic modes lie below the light line of the cladding material and are truly guided, whereas those lying above the light line are subject to intrinsic radiation losses due to out-of-plane diffraction. In addition, extrinsic factors like insufficient etch depth, roughness or nonvertical shape of the holes, and disorder may contribute to radiative losses. While the extrinsic factors may be controlled by improving the fabrication procedures, the light line problem represents an intrinsic limit for the application of PC slabs to integrated photonics. It is therefore important to quantify the level of intrinsic losses and to know their dependence on the structure parameters.

In this work we present theoretical results for intrinsic diffraction losses in PC waveguides containing line defects. We focus on the most common structure, namely the triangular lattice of air rods with a missing row of holes in the Γ - K direction or "W1 waveguide" (see inset in Fig. 1). We assume a typical system with strong refractive index contrast, namely the self-standing membrane or "air bridge."^{4,6,7,9,13} The frequency (or wave vector) dependence of the losses and the trends as a function of hole radius, channel width, and membrane thickness are quantitatively addressed.

We consider a slab waveguide with core thickness d in the vertical (z) direction and a periodic patterning in the xy plane: each layer j is characterized by a dielectric constant $\epsilon_j(x,y)$. The theoretical method relies on an expansion of the magnetic field on the basis of guided modes of an effective waveguide, where each layer is taken to have a homogeneous dielectric constant given by the spatial average of $\epsilon_j(x,y)$.¹⁴ The free waveguide modes are folded in the first Brillouin zone and are coupled by the off-diagonal components of the inverse dielectric tensor. Results for the frequency dispersion of photonic modes and for the gap maps of two-dimensional (2D) PC slab structures are shown in Ref. 14. In order to calculate diffraction losses, coupling of quasiguided modes above the light line with radiative modes

of the effective waveguide is here taken into account by Fermi's golden rule. The present method goes beyond the nearly free photon approximation of Ref. 11 since the dielectric patterning is treated in a nonperturbative way. Results for the imaginary part of the frequency of photonic modes are found to agree with those calculated by finite-difference time-domain simulations in three dimensions.¹⁰

In Fig. 1 we show the dispersion of photonic modes for a W1 waveguide in an air bridge with dielectric constant $\epsilon = 12$ and core thickness $d = 0.3a$, patterned with a triangular lattice of holes with radius $r = 0.36a$, where a is the lattice constant.¹⁷ Only modes which are even with respect to reflection in the horizontal midplane ($\sigma_{xy} = +1$) and odd with respect to reflection in the vertical midplane of the channel ($\sigma_{kz} = -1$) are shown.^{5,7,11} The gap of the triangular lattice forms between 0.33 and 0.47 (in terms of the dimensionless frequency $\omega a / (2\pi c) = a/\lambda$) and the modes in the gap associated with the linear defect can be recognized: they are marked as α for the index-confined mode, and β for the

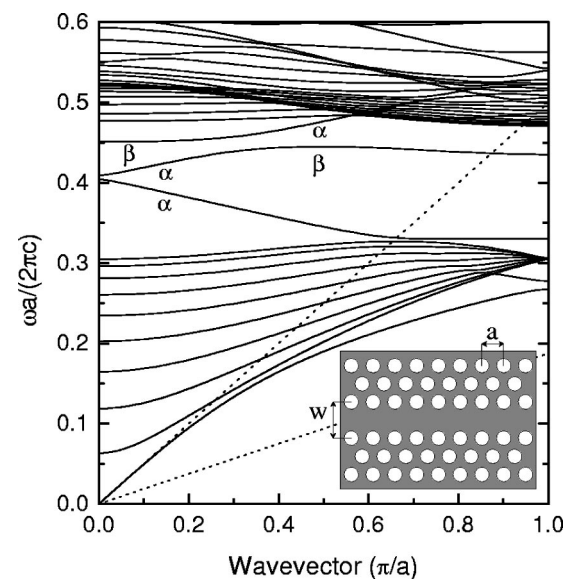


FIG. 1. Dispersion of photonic modes for a W1 linear waveguide in an air bridge of thickness $d = 0.3a$ and dielectric constant $\epsilon = 12$. The hole radius is $r = 0.36a$. The dotted lines denote the light dispersion in the core material and in air. The inset shows the 2D structure in real space: for a W1 waveguide, $w = w_0 = \sqrt{3}a$.

^{a)}Author to whom correspondence should be addressed; electronic mail: andreani@fisicavolta.unipv.it

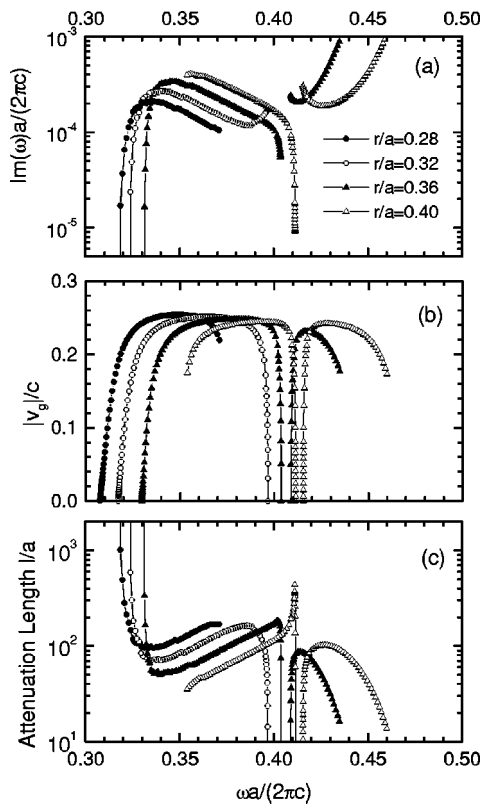


FIG. 2. (a) Imaginary part of the energy, (b) group velocity, (c) attenuation length of the lowest guided modes for a W1 linear waveguide in an air bridge with $d=0.3a$ and $\epsilon=12$, for different hole radii. The results are plotted only for the energies for which the waveguide is monomode.

gap-confined mode.⁵ Notice the mini-stop band in the α mode at $k=0$ around $a/\lambda=0.405$, and a higher one at $k \neq 0$ between α and β modes.^{3,7,13} The lowest mode lies above the light line in air for about 2/3 of the Brillouin zone, then it crosses the light line and it becomes truly guided, albeit with a very low group velocity. The group velocity in the guided mode region can be increased by a careful structure design.¹² In this work we are not concerned with this issue, nor with the problem of having a region of monomode waveguide propagation when modes of both vertical parities ($\sigma_{k_z} = \pm 1$) are considered.^{7,13}

In Fig. 2 we show (a) the imaginary part of the frequency, (b) the modulus of the group velocity $|v_g|/c$ and (c) the attenuation length ℓ/a : the latter is defined as $\ell^{-1} = 2|\text{Im}(k)|$, where the imaginary part of the wave vector is given by $\text{Im}(k) = \text{Im}(\omega)/v_g$. These quantities are plotted as a function of frequency in the photonic gap, for the same air bridge structure of Fig. 1, but for increasing values of the hole radius. For the sake of clarity, the results are shown only when the channel waveguide is monomode for the specified parity. As a first remark, the imaginary part of the frequency is between 10^{-3} and 10^{-4} , i.e., much smaller than in periodic 2D lattices:¹⁰ this is due to lateral field confinement in the dielectric channel, which reduces the overlap with the patterned regions where radiative losses occur. The losses increase with the air fraction in the lattice, as expected from previous theoretical models² and experimental results.^{9,15} The losses go to zero at the lowest edge of the mode dispersion window, where the mode crosses the light line (see Fig. 1). For all investigated cases, there is a frequency region

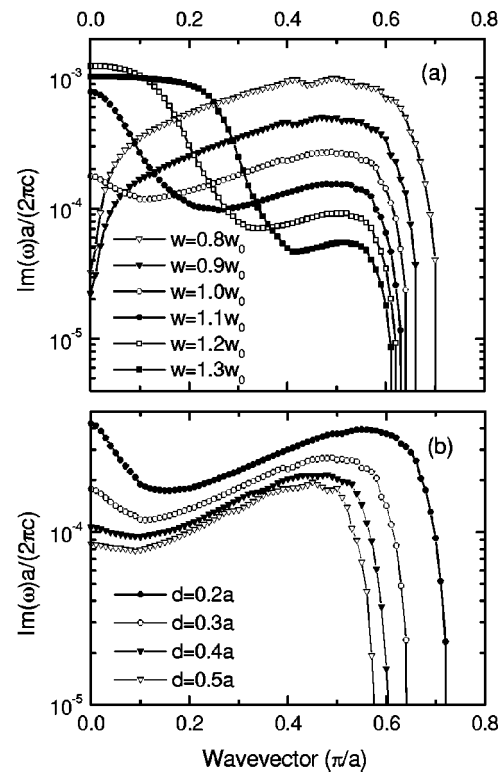


FIG. 3. Imaginary part of the energy of the lowest guided mode for a linear waveguide in an air bridge with $\epsilon=12$, hole radius $r=0.32a$, (a) for a core thickness $d=0.3a$ and different values of the channel width w , or (b) for a channel thickness $w=w_0$ and different values of the core thickness d .

where the mode dispersion is linear with a group velocity v_g close to c/n , where n is an average refractive index of the mode. The attenuation length depends smoothly on frequency when v_g is close to c/n . The results of Fig. 2(c) show that the typical attenuation length of a W1 waveguide in the air bridge is of the order of 10^2 lattice constants (e.g., $\sim 50 \mu\text{m}$ at $\lambda = 1.5 \mu\text{m}$). For $r/a=0.36$ and 0.40 a mini-stop band can be recognized around $a/\lambda \sim 0.4-0.42$. At the edge of the mini-stop band $\text{Im}(\omega)$ always tends to a finite constant: in other words, even at $k=0$ there are active diffraction channels for radiative losses. The opposite curvature of the lower and upper modes at the mini-gap edge for $r/a=0.36$ and 0.40 can be related to the opposite parities of the two modes with respect to a vertical mirror plane perpendicular to the channel. Since v_g vanishes at the mini-gap edge, the attenuation length must also vanish there. However, Fig. 2(c) shows that the attenuation length first increases when the energy approaches the mini-gap edge from below, then it decreases towards zero in a frequency range which can be extremely narrow.

Since the diffraction losses depend on the extension of the electromagnetic mode in the patterned regions, it is worthwhile to study the behavior of the losses as a function of the channel width w as defined in the inset of Fig. 1 ($w = w_0 \equiv \sqrt{3}a$ for the W1 waveguide) or as a function of the core thickness d . This is illustrated in Fig. 3, which shows $\text{Im}(\omega)$ as a function of the wave vector for $r/a=0.32$, when the channel width increases from $0.8w_0$ to $1.3w_0$ at fixed $d=0.3a$ [Fig. 3(a)] and when the core thickness increases from $0.2a$ to $0.5a$ at fixed channel width $w=w_0$ [Fig. 3(b)]. In both cases, far enough from the mini-gap clear trends can

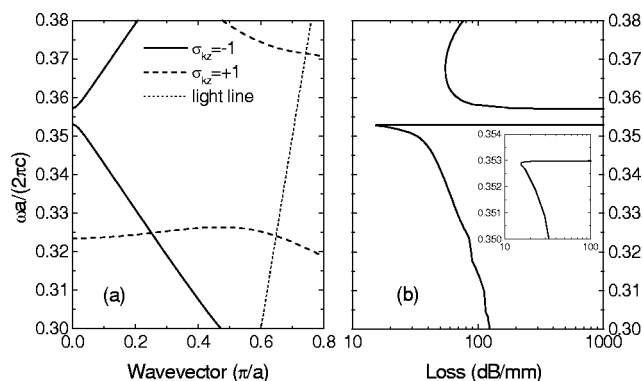


FIG. 4. (a) Defect mode dispersion and (b) propagation loss of the $\sigma_{kz} = -1$ modes for the parameters of the Si slab measured in Ref. 13: $a = 530$ nm, $r/a = 0.392$, $d/a = 0.566$, $\epsilon = 12.25$.

be recognized: the intrinsic losses decrease on increasing either the channel width or the core thickness, due to an increased lateral confinement of the defect mode. The reduction of the losses is particularly pronounced (more than one order of magnitude) for the case of the channel width dependence.¹⁸ On approaching the mini-gap at $k=0$, the wave vector-dependence of $\text{Im}(\omega)$ becomes more complicated and is found to depend critically on the channel width w : in some cases $\text{Im}(\omega)$ decreases, while in other cases it increases when $k \rightarrow 0$. This may be explained by mixing of the dielectric defect mode α with the higher-lying gap-confined mode β (see Fig. 1), this mixing being very sensitive to small changes in structure parameters.

Finally, in Fig. 4 we present the calculated mode dispersion and losses for the parameters of the experiment of Ref. 13, which was performed on a Si slab. Figure 4(a) displays the dispersion of both odd ($\sigma_{kz} = -1$) and even ($\sigma_{kz} = +1$) modes with respect to vertical parity. Figure 4(b) shows the propagation loss $(10 \log_{10} e) l^{-1}$ of the $\sigma_{kz} = -1$ modes. On approaching the mini-gap edge, the loss of the lowest mode decreases substantially, in agreement with the experimental results.¹³ The inset in Fig. 4(b) shows that the upturn of the losses close to the lower mini-gap edge [as in Fig. 2(c)] occurs in a frequency window that is too narrow to be relevant for the experiment. The loss for $a/\lambda = 0.33$ is close to that calculated in Ref. 13 with the finite-difference time-domain method. It would be interesting to perform loss measurements for the upper mode, which we predict to have *increasing* loss on approaching the mini-gap from above.

The present approach is a fast and accurate method for calculating *intrinsic* losses and as such it is particularly suited to study the trends as a function of the various parameters. When the group velocity is constant and close to c/n ,

the losses depend smoothly on frequency and have clear trends as a function of structure parameters: the diffraction losses increase with the air fraction in the 2D lattice and decrease rapidly on increasing the width of the channel or the slab thickness. The same trends are expected to hold for losses due to other scattering processes, i.e., for *extrinsic* losses related to disorder and fabrication-induced defects. Both the imaginary part of the frequency and the propagation losses have a complex behavior as a function of frequency, particularly on approaching a mini-gap between modes. Good agreement with the frequency dependence of the losses measured by Lončar *et al.*¹³ is found.

Useful discussions with J.-P. Albert and M. Le Vassor d'Yerville are gratefully acknowledged. This work was supported by MIUR through the Cofin program and by INFN through PRA "PHOTONIC."

- ¹T. F. Krauss, R. M. De La Rue, and S. Brand, *Nature (London)* **383**, 699 (1996).
- ²H. Benisty, D. Labilloy, C. Weisbuch, C. J. M. Smith, T. F. Krauss, D. Cassagne, A. Béraud, and C. Jouanin, *Appl. Phys. Lett.* **76**, 532 (2000).
- ³C. J. M. Smith, H. Benisty, S. Olivier, M. Rattier, C. Weisbuch, T. F. Krauss, R. M. De La Rue, R. Houdré, and U. Oesterle, *Appl. Phys. Lett.* **77**, 2813 (2000).
- ⁴E. Chow, S. Y. Lin, S. G. Johnson, P. R. Villeneuve, J. D. Joannopoulos, J. R. Wendt, G. A. Vawter, W. Zubrzycki, H. Hou, and A. Alleman, *Nature (London)* **407**, 983 (2000).
- ⁵S. G. Johnson, P. R. Villeneuve, S. Fan, and J. D. Joannopoulos, *Phys. Rev. B* **62**, 8212 (2000).
- ⁶T. Baba, A. Motegi, T. Iwai, N. Fukaya, Y. Watanabe, and A. Sakai, *IEEE J. Quantum Electron.* **38**, 743 (2002).
- ⁷X. Letartre, C. Seassal, C. Grillet, P. Rojo-Romeo, P. Viktorovitch, M. Le Vassor d'Yerville, D. Cassagne, and C. Jouanin, *Appl. Phys. Lett.* **79**, 2312 (2001).
- ⁸Ph. Lalanne and H. Benisty, *J. Appl. Phys.* **89**, 1512 (2001).
- ⁹N. Kawai, K. Inoue, N. Carlsson, N. Ikeda, Y. Sugimoto, K. Asakawa, and T. Takemori, *Phys. Rev. Lett.* **86**, 2289 (2001).
- ¹⁰T. Ochiai and K. Sakoda, *Phys. Rev. B* **63**, 125107 (2001).
- ¹¹T. Ochiai and K. Sakoda, *Phys. Rev. B* **64**, 045108 (2001).
- ¹²M. Notomi, A. Shinya, K. Yamada, J. Takahashi, C. Takahashi, and I. Yokohama, *IEEE J. Quantum Electron.* **38**, 736 (2002).
- ¹³M. Lončar, D. Nedeljković, T. P. Pearsall, J. Vučković, A. Scherer, S. Kuchinsky, and D. C. Allan, *Appl. Phys. Lett.* **80**, 1689 (2002).
- ¹⁴L. C. Andreani and M. Agio, *IEEE J. Quantum Electron.* **38**, 891 (2002).
- ¹⁵M. Patrini, M. Galli, F. Marabelli, M. Agio, L. C. Andreani, D. Peyrade, and Y. Chen, *IEEE J. Quantum Electron.* **38**, 885 (2002).
- ¹⁶A. Yariv, *Opt. Lett.* **27**, 936 (2002).
- ¹⁷The calculation employs a supercell with a periodicity of $8w_0 + w$; 535 plane waves and four guided modes are used in the basis set. For the loss calculations, an average of the results with supercell widths from $3w_0 + w$ up to $8w_0 + w$ is taken in order to smooth out finite supercell effects.
- ¹⁸We do not obtain any "quantized" low-loss values for the channel thickness, as predicted by coupled-mode theory.¹⁶ Indeed, the present parameters are far from those assumed in Ref. 16, where the refractive index modulation is assumed to be small compared to the average value.